

Modeling the Kinetics of Pyrolysis of Date Seeds Using Artificial Neural Networks

R.A. Felobes¹ and M.F. Abadir²

¹ The Chemical Engineering Department – Higher Technological Institute – 10th of Ramadan, Egypt

² The Chemical Engineering Department – Faculty of Engineering – Cairo University, Giza, Cairo, Egypt

rahmaadel613@gmail.com, magdi.abadir@eng.cu.edu.eg

ABSTRACT

Ground date seeds were subjected to thermal analysis in a stream of Nitrogen at four different heating rates (5, 10, 15 and 20°C.min⁻¹) and their TG – DTG patterns were obtained. Two peaks showed up for the degradation of lignocellulosic components. Three iso-conversional methods were used to obtain the activation energy of these steps: the Flynn-Wall-Ozawa (FWO), the Kissinger-Asahira-Sunozé (KAS) and the Friedmann methods. The results show that the values of activation energy for the first step of degradation varied from 113.76 to 117.80 kJ.mol⁻¹, depending on the calculation method. For the second step, the corresponding values were 130.99, 123.07 and 127.52 kJ.mol⁻¹. At the end of the second peak, biochar was formed that went on cracking off its more volatile constituents at higher temperatures. An artificial Neural Network simulation was carried out for the first degradation step. The values obtained from that simulation for conversion – temperature curves and for biochar content were in excellent agreement with the corresponding experimental figures. However, the simulated values obtained for activation energy at different conversion levels were higher.

Index-words: Activation energy, ANN Simulation, Conversion, Date seeds, Percent biochar, Pyrolysis.

I. INTRODUCTION

Substituting fossil fuels by waste in many industrial fields has become an increasingly common practice in the last two decades to alleviate some of the effects of the continuous depletion of fossil fuel type [1, 2]. A typical example is the partial use of some agricultural waste in the firing process in the cement industry [3, 4]. In this context, biorefineries using agricultural and food waste are considered a sustainable energy source [5].

On the other hand, pyrolysis of vegetable and food waste has proved to be a rich source of gaseous, and liquid and solid products that possess many uses, among which is substituting fossil fuels. Slow pyrolysis of agricultural waste at heating rates not exceeding 80°C.min⁻¹ results in the formation of biochar, which possesses an elevated calorific value [6 – 8], besides exhibiting a large surface area for use as adsorbent in wastewater treatment [9 – 11]. Faster pyrolysis at rates reaching 1000°C.min⁻¹ normally yields biooil rather than solid biochar, which is largely used as a promising substitute for conventional fuels [12, 13] and as cosmetic material

[14]. The production of bio-oil can be enhanced using flash pyrolysis at heating rates exceeding 1000°C.min⁻¹ [15, 16].

Research involving disclosure of the mechanism of slow pyrolysis of agricultural waste has yielded abundant literature in which most authors agreed on a common mechanism of waste degradation [17 – 21]. This consists of elimination of moisture followed by devolatilization of lignocellulosic material (Hemi-cellulose, cellulose, and lignin) and ends at a temperature ~400°C by forming biochar. At higher temperatures, the final elimination of lignin takes place as well as cracking of the formed biochar. The kinetics of such devolatilization reactions have been followed up by thermal analysis. This technique involves either following up the change in weight with time at constant temperature, or heating at constant heating rates. The former method can only be used whenever the conditions of reaction are isothermal [22, 23] which is hardly the case in pyrolysis reactions. That is why kinetics of these processes are commonly studied at constant heating rates usually using non – model kinetic techniques, the most common of which were the Flynn – Wall

- Ozawa (FWO), the Kissinger - Asahira - Sunose (KAS) and the Friedman techniques. These models yield the value of activation energy of the reactions occurring on pyrolysis without generally specifying the controlling step [24 - 29]. On the other hand, model fitting methods that disclose the reaction's controlling step have only been successfully used whenever the reaction was well - defined [28, 27], which is not usually the case in pyrolyzing agricultural waste [30, 31]. Nevertheless, whenever the most used model fitting method, namely the Coats - Redfern model, was used most devolatilization reactions of lignocellulosic components turned out to follow first order kinetics [32, 33].

Attempts to model the degradation of agricultural waste using mathematical analysis were limited owing to the complexity of the reactions thereof. Using a kinetic analysis of simultaneous reactions, Sheth and Babu [34] studied the pyrolysis of wood and obtained model results which reasonably agree with experimental outcome. A similar approach was recently presented by Bieniek et al. on studying the pyrolysis of brewery spent grain and medium-density fiberboard [35]. On the other hand, several researchers have used simulation techniques, such as ANN (Artificial Neural Networks), to model the degradation kinetics of different types of biomasses [36 - 39].

In particular, the kinetics of pyrolysis of date seeds were investigated by Aly et al. [40]. They used several model and non-model methods to evaluate the activation energy of degradation of lignocellulosic components and obtained values of activation energy ranging from 135 to 160 kJ.mol⁻¹ depending on the technique used in calculations. On the other hand, Raza et al. [41] used the Coats - Redfern technique to obtain a value of activation energy ranging from 170 to 190 kJ.mol⁻¹, depending on the heating rate used, a result close to that obtained by Aly et al. [40].

In the present paper, the kinetic parameters of the pyrolysis of date seeds were determined using three different iso-conversional methods, and the results were compared to those obtained using Artificial Neural Networks (ANN) modelling. The use of ANN simulation is a step towards further use of that simulation technique to predict the different outcomes of degradation of agricultural waste since no mathematical tool can easily deal with the kinetics of the complex reactions occurring thereof.

II. MATERIALS AND METHODS

A. Raw Material

The sole raw material used in this investigation consists of date seeds (Zaghloul type) collected from the local market in Cairo, Egypt. These were ground and screened between sieves 16 (0.792 mm) and 20 (0.635 mm) as per ASTM C136-01 [42], with an average particle size = 0.714 mm. The ash content of the ground powder was determined by heating samples of powder to 1000°C. An average ash content of 0.62% was obtained.

B. Thermal Analysis

This was conducted at four different heating rates (5, 10, 15 and 20°C.min⁻¹) using about 15 mg of ground material, dried overnight in a muffle dryer at 80°C. Nitrogen was admitted to the apparatus (Universal V4.5A TA Instruments) at the rate of 50mg.min⁻¹. Conversion in the main step of the devolatilization of lignocellulosic components was calculated using the expression:

$$\alpha = \frac{m_0 - m}{m_0 - m_f} \quad (1)$$

Where:

- m_0 represents the initial mass before decomposition.
- m represents the mass after any time along the decomposition reaction.
- m_f represents the final mass left after decomposition.

C. Calculation Models

As previously pointed out, non-model techniques are more reliable in determining the kinetic parameters of degradation of lignocellulosic materials. For that reason, three methods were chosen to that aim.

1. Flynn - Wall - Ozawa (FWO) method

This method relies on integrating the basic kinetic equation:

$$\frac{d\alpha}{dt} = A e^{-\frac{E}{RT}} f(\alpha) \quad (2)$$

Where:

- A is a pre-exponential factor (s⁻¹)
- E is the activation energy for reaction (J.mol⁻¹)
- R is the general gas constant (J.mol⁻¹K⁻¹)
- T is the temperature (K)

$f(\alpha)$ is a function of conversion that depends on the rate controlling step.

Considering the rate of heating to be $\beta = \frac{dT}{dt}$ °C.min⁻¹, Equation (2) can be written as:

$$\frac{d\alpha}{dT} = \frac{A}{\beta} e^{-\frac{E}{RT}} f(\alpha) \quad (3)$$

Separation of variables and integrating, the following expression is obtained:

$$\frac{A}{\beta} \int e^{-\frac{E}{RT}} dT = \int \frac{d\alpha}{f(\alpha)} \quad (4)$$

The LHS cannot be integrated analytically, and requires expanding the integrand into an infinite series, of which only the first terms are kept. The final expression takes the form:

$$\log \beta = \ln \frac{A f(\alpha)}{\frac{d\alpha}{dT}} - \frac{E}{0.4567RT} \quad (5)$$

Hence, a plot of $\log \beta$ against $1/T$ should yield, for each value of conversion α , a straight line of slope

$\frac{E}{0.4567R}$ from which the activation energy can be calculated, at each value of α .

2. Kissinger - Asahira - Sunoze (KAS) method

This method is a generalization of the classical Kissinger method [43]. The original method was based on DTG peak having an inflection point of the $\alpha-T$ curve. It was later modified to suit any conversion, and not necessarily that at inflection.

The final kinetic equation takes the form:

$$\ln \frac{\beta}{T_\alpha^2} = -\frac{E}{RT_\alpha} + \ln \frac{R A(\alpha)}{E \cdot g(\alpha)} \quad (6)$$

Here, T_α is the temperature corresponding to a conversion = α and $g(\alpha)$ is a kinetic function related to $f(\alpha)$ by the expression:

$$g(\alpha) = \int \frac{d\alpha}{f(\alpha)} \quad (7)$$

Equation 6 reveals that a plot of $\ln \frac{\beta}{T_\alpha^2}$ against $1/T$ will produce straight lines, for different values of α , of slope = $-E/R$, from which the value of E is obtained.

3. Friedman method

The merit of that method is that it involves neither assumptions nor serious approximations, as it deals with the basic kinetic equation 3, by rewriting it in the form:

$$\ln \beta \frac{d\alpha}{dT} = \ln A f(\alpha) - \frac{E}{RT} \quad (8)$$

The values of $\frac{d\alpha}{dT}$ can be obtained from the $\alpha-T$ plot by calculating $\frac{\Delta\alpha}{\Delta T}$ at small conversion intervals (0.05) and a plot of $\ln \beta \frac{\Delta\alpha}{\Delta T}$ against $1/T$ will yield straight lines, at each value of α , of slope = $-E/R$, from which the value of E can be determined.

This method can also be used to validate a rate controlling step using the concept of kinetic compensation according to which a plot of $\ln A$ against E , for different values of conversion, should yield a straight line [44]. To obtain the value of $\ln A$,

the intercepts of the $1/T - \ln \beta \frac{\Delta\alpha}{\Delta T}$ plots are first

determined at each conversion level. Their values = $\ln A f(\alpha)$. Next, a kinetic function $f(\alpha)$ is assumed from table I.

The reliability of the different iso-conversional methods used in the calculation of the kinetic parameters in degradation reactions has been the subject of much dispute, although most authors prefer using the Friedman method over the two other techniques. This is since it relies on using the basic kinetic equation (2) without making any serious assumptions. Also, it allows for the determination of the most probable controlling step of the reaction [46].

TABLE I
THE FUNCTION $f(a)$ FOR DIFFERENT RATE
CONTROLLING STEPS [45]

Designation	Controlling step	$f(a)$
A	Crystallization and grain growth (Avrami-Erofeev)	$2(1-\alpha) \cdot [\ln(1-\alpha)]^{\frac{m-1}{m}}$
F0	Zero order reaction	0
F1	First order reaction	$1-\alpha$
F _n	nth order reaction ($n \neq 1$)	$(1-\alpha)^n$
R2	Cylindrical: Reaction at interface (Shrinking cylinder)	$2(1-\alpha)^{\frac{1}{2}}$
R3	Spherical: Surface reaction at interface (Shrinking sphere)	$3(1-\alpha)^{\frac{2}{3}}$
D1	One dimensional diffusion	$\frac{1}{2}$
D2	Two-dimensional diffusion	$-\ln(1-\alpha)$
D3	Three-dimensional diffusion (Thin ash layer - Jander equation)	$\frac{3(1-\alpha)^{\frac{2}{3}}}{2-(1-\alpha)^{\frac{1}{3}}}$
D4	Spherical: diffusion through ash (Ginstling - Brounstein equation)	$\frac{1}{2 \left[(1-\alpha)^{\frac{1}{3}} - 1 \right]}$

Usually, the determination coefficients (R^2) for the plot of $\ln A$ against E is obtained for probable expressions of $f(\alpha)$, the highest value corresponding to the most probable controlling mechanism.

In general, The Friedman method is often preferred to the two other techniques since it relies on little or no assumptions, besides disclosing the most probable controlling step of the reaction.

D. Modelling Using Artificial Neural Networks (ANN)

Neural networks were used to predict the conversion, biochar yield and activation energy based on the input variables such as biomass type, heating rate, temperature, and residence time. Neural networks can also capture the non-linear and complex relationships between the input and output variables, which are often difficult to describe by conventional models [47].

In the present work, MATLAB codes for pyrolysis of biomass have been used. The conventional steps of neural networks modelling were followed [48]:

- **Collection of data:** This step consisted of gathering as much data as possible from the literature dealing with the pyrolysis of vegetable waste. This included the effect of time and/or temperature on conversion to biochar, its final yield and its composition, and the activation energy of degradation.
- **Modelling:** For pyrolysis modeling, a feedforward network was used, which is the simplest and most common type. It possesses an input layer, one or more hidden layers, and an output layer. The input layer receives the input variables, the hidden layers perform the computations, and the output layer produces the output variables.
- **Training:** This step is necessary to adjust the network weights and biases, which are the parameters that determine the network output. The learning algorithm is the method that updates the network parameters based on the error function, which measures the difference between the network output and the desired output. In the present work, backpropagation was used, which calculates the error gradient for each network parameter and updates them in the opposite direction of the gradient.
- **Validation:** This is carried out by determining statistical parameters such as root mean squared error, correlation coefficient (R), determination coefficient (R^2), etc. In the present work, the determination coefficient has been used as it measures to what extent variation of output variables relate to variation in input variables.

III. Results and Discussion

The chosen case was that corresponding to the ground material pyrolyzed at a heating rate = $10^\circ\text{C} \cdot \text{min}^{-1}$.

A. TG - DTG Results

The TG (Thermogravimetry) - DTG (Differential Thermogravimetry) curves for a specimen of powder pyrolyzed in Nitrogen at a heating rate of $10^\circ\text{C} \cdot \text{min}^{-1}$ are shown in Figure 1. There is a sharp DTG peak at 316.04°C corresponding to the devolatilization of hemicellulose and cellulose and partly lignin, as is the case for the pyrolysis of most lignocellulosic

materials [21,49]. The full devolatilization of lignin ends at about 400°C, whereby biochar is formed associated with a second DTG peak at 369.31°C. This was assessed by heating 50 g of the material in presence of Nitrogen in a muffle furnace at the same heating rate after which heating was stopped. Figure 2 displays an image of the resulting biochar.

B. Conversion - Temperature Curves for the First Degradation Step

From the spreadsheet obtained for TG data, it was possible to calculate the conversion at different temperatures corresponding to the first DTG peak at all four heating rates. Figure 3 shows the curves obtained for conversion of ground date seeds for the first decomposition step, corresponding to the first DTG peak in Figure 1.

C. Determination of Kinetic Parameters for the First Degradation Step

As previously pointed out, determination of the kinetic parameters was carried out using three different non-model methods. The results are reviewed in the following sections.

1. Application of the FWO method

When values of $\log \beta$ against $1/T$ were plotted for different conversion levels, straight lines were obtained, as evidenced from Figure 4.

From the slopes of the lines, it was possible to evaluate the activation energy at each conversion. The values and the corresponding values obtained by the two other methods are listed in Table III. The average activation energy = 116.06 kJ.mol⁻¹.

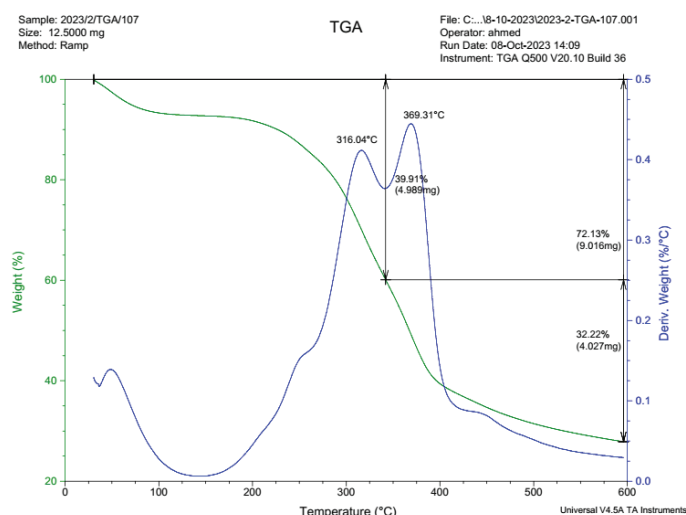


Fig. 2. Biochar prepared by firing in Nitrogen to 600°C

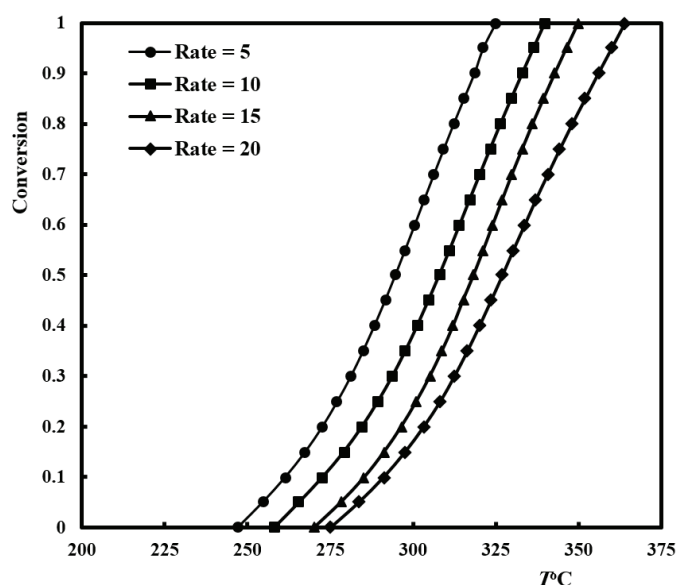


Fig. 3. Conversion - temperature curves for ground date seeds (Step 1)

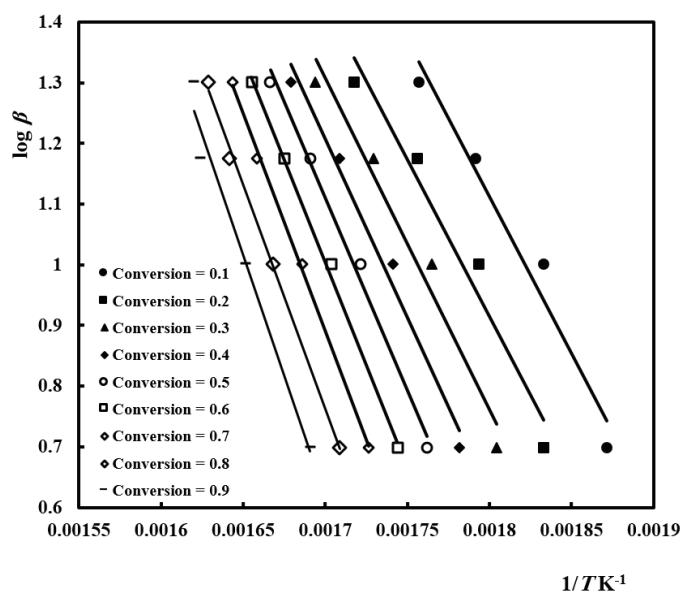


Fig. 4. FWO plots for ground date seeds (Step 1)

Fig. 1. Thermal analysis curves of ground date seeds at 10°C.min⁻¹

2. Application of the KAS method

In this method, values of $\ln \frac{\beta}{T^2}$ were plotted against $1/T$ to obtain the series of straight lines appearing in Figure 5. The average activation energy = 117.80 kJ.mol⁻¹, a value almost identical to that obtained by the previous technique.

3. Application of the Friedman method

As previously explained, plots of $\ln \beta \frac{\Delta\alpha}{\Delta T}$ against $1/T$ were carried out for different conversion levels, with an increment $\Delta\alpha = 0.05$ to obtain the set of straight lines in Figure 6. Once again, it was possible to determine the value of activation energy at each conversion. The average value of $E = 113.76$ kJ.mol⁻¹, a value slightly lower than those obtained previously.

Next, the intercepts of the lines in Figure 6 were determined and the values of $\ln Af(\alpha)$ calculated at each value of conversion. Following most previous findings, a first order reaction was assumed, having the kinetic function:

$$f(\alpha) = 1 - \alpha \quad (9)$$

This allowed plotting the values of $\ln A$ against E . A straight line was obtained (Figure 7) with $R^2 = 0.980$, assessing the validity of the proposed kinetic mechanism.

The discrepancies in the average values of activation energy obtained by different methods are a common occurrence, caused by the various assumptions made along the establishment of the kinetic model [49, 50]. A comparison of the values of activation energy obtained at different conversion levels by the three methods is given in Table II.

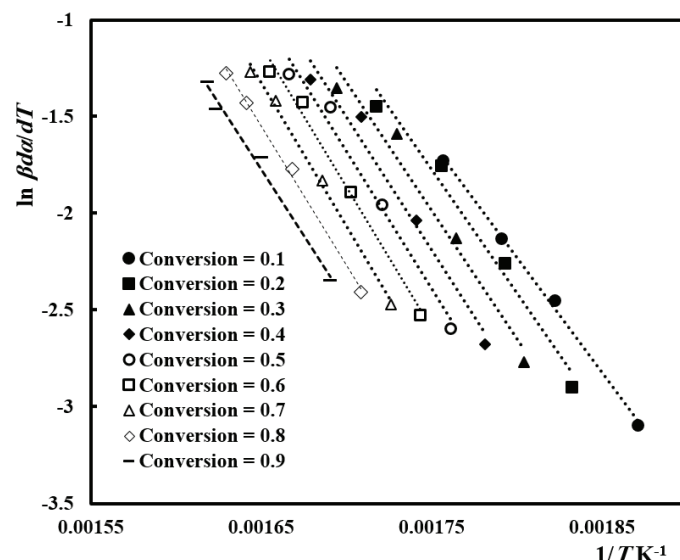


Fig. 6. Friedman plots for ground date seeds (Step 1)

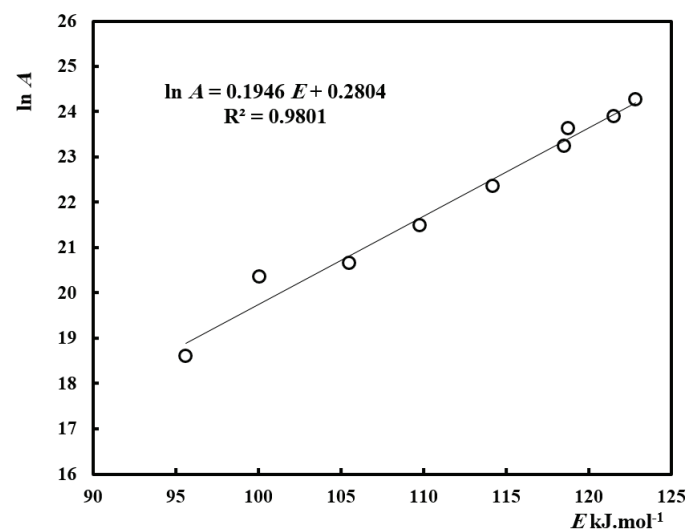


Fig. 7. Application of kinetic compensation (Step 1)

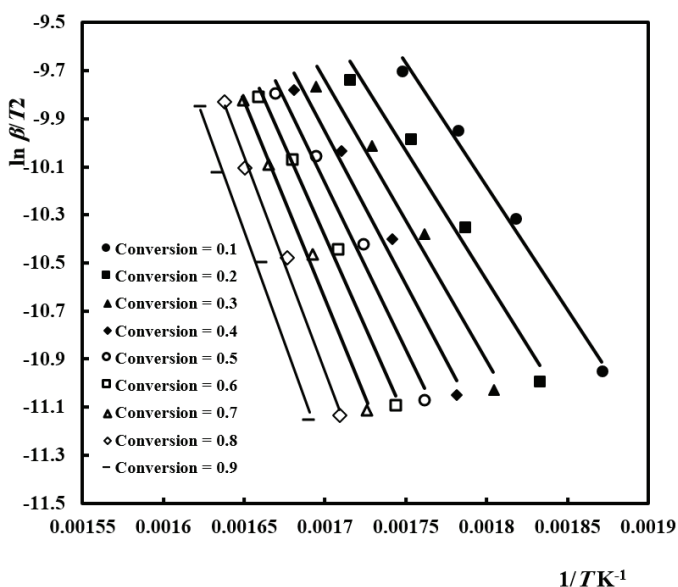


Fig. 5. KAS plots for ground date seeds (Step 1)

TABLE II
ACTIVATION ENERGIES OBTAINED BY DIFFERENT METHODS FOR DATE SEEDS (kJ.mol⁻¹)

α	0.1	0.2	0.3	0.4	0.5	0.6	0.7	0.8	0.9	Mean
FWO	94.16	94.37	99.47	106.95	115.35	123.38	130.91	134.93	144.98	116.06
KAS	85.58	89.93	96.47	105.56	115.40	126.12	137.20	148.73	155.22	117.80
Friedman	98.73	105.49	109.78	114.19	118.50	121.53	122.85	118.77	114.03	113.76

The values obtained for the activation energy using different non-model techniques are close to those obtained by Aly et al. [40], on studying the kinetics of pyrolysis of date kernels, varying from 126.5 to 145 kJ.mol⁻¹, depending on the heating rate and method of calculation, although they did not specify the particle size used in their work. The results obtained by Rasa et al. [41] (170 – 190 kJ.mol⁻¹) are less reliable, being obtained by the Coats – Redfern technique, which is unsuitable for use for complex reactions [23].

E. Conversion – Temperature Curves for the Second Degradation Step

In Figure 8, the conversion – temperature curves for the second step of the degradation of the lignocellulosic components ending by the formation of biochar are illustrated.

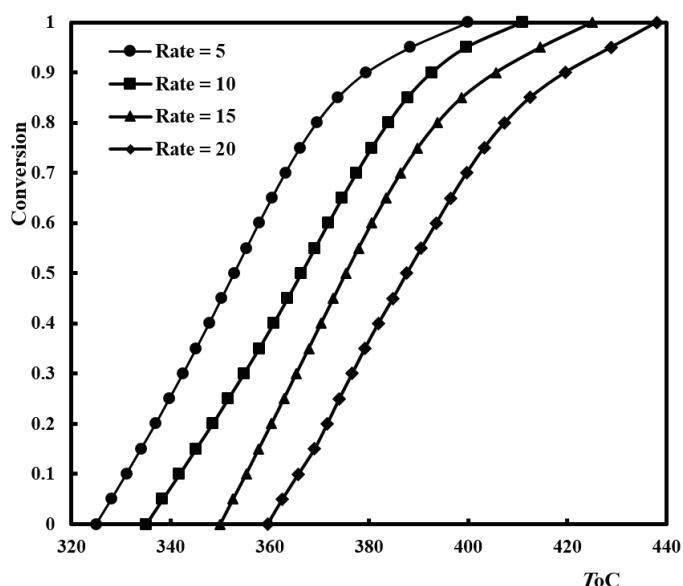


Fig. 8. Conversion – temperature curves for ground date seeds (Step 2)

F. Determination of Kinetic Parameters for the Second Degradation Step

To avoid any redundancy, only the results obtained for average activation energy, as obtained by the three techniques (FWO, KAS and Friedman), are summarized in Table III.

TABLE III
AVERAGE ACTIVATION ENERGIES FOR THE SECOND DEGRADATION STEP

Method	FWO	KAS	Friedman
E kJ.mol⁻¹	130.99	123.07	127.52

IV. RESULTS OF ARTIFICIAL NEURAL NETWORK MODELLING

A. Modelling of Conversion Curves

Conversion curves for the first degradation step were modelled using Artificial Neural Networks (ANN) and compared to experimental points. Figure 9 illustrates one instance, namely, the case of particles heated at 5°C.min⁻¹. The figure reveals an excellent match of conversion data. The Root Mean Squared Error (RMSE) between experimental and calculated conversions possessed a very low value (0.0500).

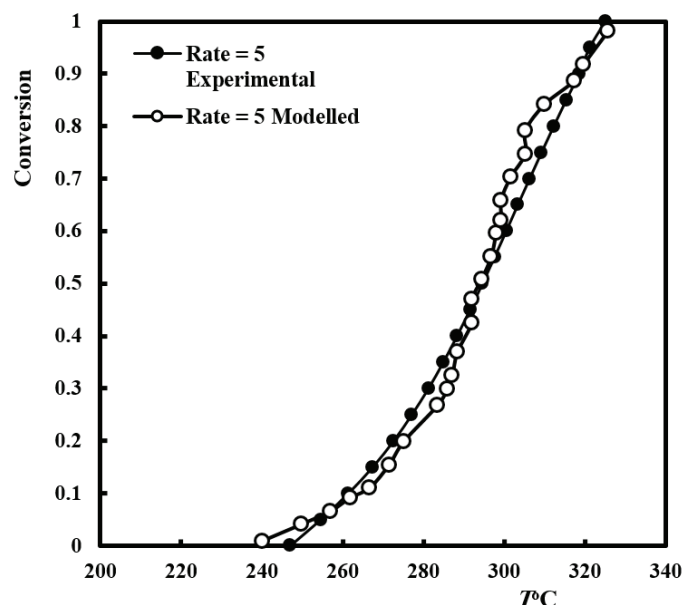


Fig. 9. Experimental and modelled data for pyrolysis at 5°C.min⁻¹

B. Biochar Yield

According to the findings of most authors [51 – 53], biochar is produced from the pyrolysis of vegetable

waste at temperatures ranging from 300 to 500°C. Its use as adsorbing material necessitates, however, increasing the temperature to more than 600°C to ensure the formation of enough porosity to allow for its use to that aim [54]. The percentage biochar formed in the present work was assessed from TG data at the temperature at which the second DTG peak ends (Figure 1). As can be seen from that figure, corresponding to pyrolysis at 10°C.min⁻¹, the second peak ends at 420°C, followed by a constant rate weight loss up to 455°C, after which the rate of weight loss slightly decreased up to 600°C. At 420°C, the total weight loss was about 62.8%, corresponding to the remaining char percentage of 36.6% (Excluding about 0.62% ash content). At 600°C, this value drops to about 22.9%. These ratios were determined at all heating rates. A comparison between the observed values and calculated values from the neural networks model at 400°C and 600°C at 10°C.min⁻¹ are shown in Table IV. The average error in the evaluation of the biochar yield, using neural network simulation is 4.76%, with a maximum of 11.65%, proving that the simulated values fairly coincide with the values determined experimentally. The root mean squared error (RMSE) was calculated and found to be 1.61 and 1.84, on comparing experimental to simulated values at 400°C and 600°C, respectively.

TABLE IV
COMPARISON BETWEEN OBSERVED AND CALCULATED
VALUES OF BIOCHAR YIELD

Heating rate °C.min ⁻¹	Biochar yield %			
	420°C		600°C	
	Observed	Simulated	Observed	Simulated
5	34.3	33.17	26.6	23.5
10	36.6	36.12	27.0	26.42
15	37.5	35.43	27.3	26.78
20	38.4	40.54	27.5	25.67
RMSE	1.61		1.84	

C. Activation Energy

The calculated values of activation energy of the first degradation step, at different levels of conversion, by the three iso-conversional models, were different but yielded very close average values. Also, it can be noticed that the first two methods resulted in an increase in activation energy while in the Friedman method, it reached a local maximum at a conversion ≈ 0.7 .

As for the values obtained from ANN simulation, they were higher than those obtained by the three

models by an average of 11.6% besides reaching a maximum value at a conversion ≈ 0.6 , as is the case with the Friedman method (Figure 10). The values of RMSE for the comparison between the results of the three methods and the simulated values were found to be 21.42 kJ.mol⁻¹, 15.29 kJ.mol⁻¹ and 7.96 kJ.mol⁻¹ for the KAS, FWO and Friedman methods respectively, proving that the results of this last method were the closest to those obtained by ANN simulation.

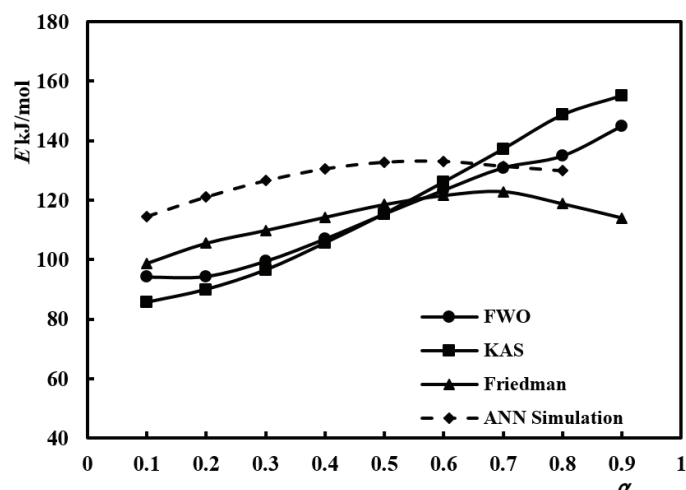


Fig. 10. Experimental and ANN simulated values of activation energy

It seems therefore, that ANN simulation could produce very close values to those determined experimentally for conversion - temperature points and biochar yield. The prediction of activation energy, however, resulted in higher results.

V. CONCLUSIONS

Date seeds were ground to an average particle size of 0.714 mm and subjected to pyrolysis in a thermal analyzer with flowing Nitrogen at four different heating rates: 5, 10, 15 and 20°C.min⁻¹. In all cases, two DTG peaks showed up associated with the devolatilization of lignocellulosic components.

Activation energies were calculated for the two degradation steps by three different iso-conversional methods, namely the Flynn - Wall - Ozawa, the Kissinger - Asahira - Sunoze and the Friedman methods. The calculated values showed slight variations between the three methods. For the first degradation step, these values were respectively 116.06, 117.80 and 113.76 kJ.mol⁻¹, while for the second step, the obtained values were: 130.99, 123.07 and 127.52 kJ.mol⁻¹.

ANN simulation was carried out for the first degradation step and the simulated values for conversion - temperature curves and biochar yield

at 420°C and 600°C were in excellent agreement with experimentally obtained values, resulting in low values of RMSE between experimental and simulated data. On the other hand, simulated values for activation energies showed moderate deviation from those calculated by the three iso-conversional methods. In particular, the Friedman method gave the minimum RMSE between experimental and

simulated data among the three methods.

It is recommended to extend ANN simulation to predict the proportion of the lignocellulosic components of various agricultural waste as well as the effect of particle size on the different pyrolysis parameters.

References

- [1] M. V. L. Chhandama, A. C. Chetia, K. B. Satyan, Supongsena Ao, J. V. Ruatpuia, and S. L. Rokhum, "Valorisation of food waste to sustainable energy and other value-added products: A review," *Bioresour Technol Rep*, vol. 17, p. 100945, Feb. 2022, doi: 10.1016/j.biteb.2022.100945.
- [2] A. Sridhar, A. Kapoor, P. Senthil Kumar, M. Ponnuchamy, S. Balasubramanian, and S. Prabhakar, "Conversion of food waste to energy: A focus on sustainability and life cycle assessment," *Fuel*, vol. 302, p. 121069, Oct. 2021, doi: 10.1016/j.fuel.2021.121069.
- [3] W. Zieri and I. Ismail, "Alternative Fuels from Waste Products in Cement Industry," in *Handbook of Ecomaterials*, Cham: Springer International Publishing, 2019, pp. 1183–1206. doi: 10.1007/978-3-319-68255-6_142.
- [4] N. Chatziaras, C. S. Psomopoulos, and N. J. Themelis, "Use of waste derived fuels in cement industry: a review," *Management of Environmental Quality: An International Journal*, vol. 27, no. 2, pp. 178–193, Mar. 2016, doi: 10.1108/MEQ-01-2015-0012.
- [5] A. Sarker, R. Ahmmed, S. M. Ahsan, J. Rana, M. K. Ghosh, and R. Nandi, "A comprehensive review of food waste valorization for the sustainable management of global food waste," *Sustainable Food Technology*, vol. 2, no. 1, pp. 48–69, 2024, doi: 10.1039/D3FB00156C.
- [6] F. Ronsse, S. van Hecke, D. Dickinson, and W. Prins, "Production and characterization of slow pyrolysis biochar: influence of feedstock type and pyrolysis conditions," *GCB Bioenergy*, vol. 5, no. 2, pp. 104–115, Mar. 2013, doi: 10.1111/gcbb.12018.
- [7] N. Cai, H. Zhang, J. Nie, Y. Deng, and J. Baeyens, "Biochar from Biomass Slow Pyrolysis," *IOP Conf Ser Earth Environ Sci*, vol. 586, no. 1, p. 012001, Oct. 2020, doi: 10.1088/1755-1315/586/1/012001.
- [8] M. Maniscalco, G. Infurna, G. Caputo, L. Botta, and N. Tz. Dintcheva, "Slow Pyrolysis as a Method for Biochar Production from Carob Waste: Process Investigation and Products' Characterization," *Energies (Basel)*, vol. 14, no. 24, p. 8457, Dec. 2021, doi: 10.3390/en14248457.
- [9] P. Srivatsav, B. S. Bhargav, V. Shanmugasundaram, J. Arun, K. P. Gopinath, and A. Bhatnagar, "Biochar as an Eco-Friendly and Economical Adsorbent for the Removal of Colorants (Dyes) from Aqueous Environment: A Review," *Water (Basel)*, vol. 12, no. 12, p. 3561, Dec. 2020, doi: 10.3390/w12123561.
- [10] B. Qiu, X. Tao, H. Wang, W. Li, X. Ding, and H. Chu, "Biochar as a low-cost adsorbent for aqueous heavy metal removal: A review," *J Anal Appl Pyrolysis*, vol. 155, p. 105081, May 2021, doi: 10.1016/j.jaap.2021.105081.
- [11] N. Jagadeesh and B. Sundaram, "Adsorption of Pollutants from Wastewater by Biochar: A Review," *Journal of Hazardous Materials Advances*, vol. 9, 2023, doi: 10.1016/j.hazadv.2022.100226.
- [12] C. L. Yiin, S. Yusup, P. Udomsap, B. Yoosuk, and S. Sukkasi, "Stabilization of Empty Fruit Bunch (EFB) derived Bio-oil using Antioxidants," 2014, pp. 223–228. doi: 10.1016/B978-0-444-63456-6.50038-7.
- [13] Y. Y. Chong, S. Gan, L. Y. Lee, H. K. Ng, and S. Thangalazhy-Gopakumar, "Role of catalysts in biofuel production through fast pyrolysis," in *Bioenergy Engineering*, Elsevier, 2023, pp. 115–132. doi: 10.1016/B978-0-323-98363-1.00023-5.
- [14] S. Bielfeldt *et al.*, "Observer-blind randomized controlled study of a cosmetic blend of safflower, olive and other plant oils in the improvement of scar and striae appearance," *Int J Cosmet Sci*, vol. 40, no. 1, pp. 81–86, Feb. 2018, doi: 10.1111/ics.12438.
- [15] O. Onay and O. M. Kockar, "Slow, fast and flash

- pyrolysis of rapeseed," *Renew Energy*, vol. 28, no. 15, pp. 2417–2433, Dec. 2003, doi: 10.1016/S0960-1481(03)00137-X.
- [16] J. O. Ighalo et al., "Flash pyrolysis of biomass: a review of recent advances," *Clean Technol Environ Policy*, vol. 24, no. 8, pp. 2349–2363, Oct. 2022, doi: 10.1007/s10098-022-02339-5.
- [17] C. Gai, Y. Dong, and T. Zhang, "The kinetic analysis of the pyrolysis of agricultural residue under non-isothermal conditions," *Bioresour Technol*, vol. 127, pp. 298–305, Jan. 2013, doi: 10.1016/j.biortech.2012.09.089.
- [18] A. Saffe, A. Fernandez, M. Echegaray, G. Mazza, and R. Rodriguez, "Pyrolysis kinetics of regional agro-industrial wastes using isoconversional methods," *Biofuels*, vol. 10, no. 2, pp. 245–257, Mar. 2019, doi: 10.1080/17597269.2017.1316144.
- [19] M. Nour, M. Amer, A. Elwardany, A. Attia, X. Li, and S. Nada, "Pyrolysis, kinetics, and structural analyses of agricultural residues in Egypt: For future assessment of their energy potential," *Clean Eng Technol*, vol. 2, p. 100080, Jun. 2021, doi: 10.1016/j.clet.2021.100080.
- [20] R. K. Mishra, S. U. Naik, S. M. Chistie, V. Kumar, and A. Narula, "Pyrolysis of agricultural waste in a thermogravimetric analyzer: Studies of physicochemical properties, kinetics behaviour, and gas compositions," *Mater Sci Energy Technol*, vol. 5, pp. 399–410, 2022, doi: 10.1016/j.mset.2022.09.001.
- [21] N. Madany, M. Gadalla, F. Ashour, and M. Abadir, "Investigating the kinetic parameters in the thermal analysis of joboba cake," *Egypt J Chem*, vol. 0, no. 0, pp. 0–0, Oct. 2022, doi: 10.21608/ejchem.2022.160576.6924.
- [22] S. T. Aly, Sh. K. Amin, S. A. El Sherbiny, and M. F. Abadir, "Kinetics of isothermal oxidation of WC-20Co hot-pressed compacts in air," *J Therm Anal Calorim*, vol. 118, no. 3, pp. 1543–1549, Dec. 2014, doi: 10.1007/s10973-014-4044-4.
- [23] R. Ebrahimi-Kahrizsangi and M. H. Abbasi, "Evaluation of reliability of Coats-Redfern method for kinetic analysis of non-isothermal TGA," *Transactions of Nonferrous Metals Society of China*, vol. 18, no. 1, pp. 217–221, Feb. 2008, doi: 10.1016/S1003-6326(08)60039-4.
- [24] A. C. R. Lim, B. L. F. Chin, Z. A. Jawad, and K. L. Hii, "Kinetic Analysis of Rice Husk Pyrolysis Using Kissinger-Akahira-Sunose (KAS) Method," *Procedia Eng*, vol. 148, pp. 1247–1251, 2016, doi: 10.1016/j.proeng.2016.06.486.
- [25] B. Khiari, M. Massoudi, and M. Jeguirim, "Tunisian tomato waste pyrolysis: thermogravimetry analysis and kinetic study," *Environmental Science and Pollution Research*, vol. 26, no. 35, pp. 35435–35444, Dec. 2019, doi: 10.1007/s11356-019-04675-4.
- [26] F. Zaman, Z. Du, A. Munawar, M. W. Ishaq, and Y. Guan, "Pyrolysis kinetics and conversion of pomegranate peels into porous carbon," *Environ Prog Sustain Energy*, vol. 42, no. 5, Sep. 2023, doi: 10.1002/ep.14153.
- [27] M. M. Alashmawy, H. S. Hassan, S. A. Ookawara, and A. E. Elwardany, "Thermal decomposition characteristics and study of the reaction kinetics of tea-waste," *Biomass Convers Biorefin*, vol. 13, no. 11, 2023, doi: 10.1007/s13399-023-04017-y.
- [28] F. Demir, B. Dönmez, H. Okur, and F. Sevim, "Calcination Kinetic of Magnesite from Thermogravimetric Data," *Chemical Engineering Research and Design*, vol. 81, no. 6, pp. 618–622, Jul. 2003, doi: 10.1205/026387603322150462.
- [29] Fedunik-Hofman, Bayon, and Donne, "Comparative Kinetic Analysis of CaCO₃/CaO Reaction System for Energy Storage and Carbon Capture," *Applied Sciences*, vol. 9, no. 21, p. 4601, Oct. 2019, doi: 10.3390/app9214601.
- [30] P. E. Sánchez-Jiménez, L. A. Pérez-Maqueda, A. Perejón, and J. M. Criado, "Limitations of model-fitting methods for kinetic analysis: Polystyrene thermal degradation," *Resour Conserv Recycl*, vol. 74, pp. 75–81, May 2013, doi: 10.1016/j.resconrec.2013.02.014.
- [31] H. Mahmood, A. Shakeel, A. Abdullah, M. Khan, and M. Moniruzzaman, "A Comparative Study on Suitability of Model-Free and Model-Fitting Kinetic Methods to Non-Isothermal Degradation of Lignocellulosic Materials," *Polymers (Basel)*, vol. 13, no. 15, p. 2504, Jul. 2021, doi: 10.3390/polym13152504.
- [32] A. Dhaundiyal, S. B. Singh, M. M. Hanon, and R. Rawat, "Determination of Kinetic Parameters for the Thermal Decomposition of Parthenium hysterophorus," *Environmental and Climate Technologies*, vol. 22, no. 1, pp. 5–21, Feb. 2018, doi: 10.1515/rtuct-2018-0001.
- [33] hanaa abdelhady, magdi Abadir, H. Sibak, and jasmine abdelraouf, "Kinetics of pyrolysis of water hyacinth: A novel empirical approach," *Egypt J Chem*, vol. 0, no. 0, pp. 0–0, Mar. 2022,

- doi: 10.21608/ejchem.2022.125143.5565.
- [34] P.N. Sheth and B.V. Babu, "Kinetic modeling of the pyrolysis of biomass" National Conference on Environmental Conservation (NCEC-2006), BITS-Pilani," https://www.researchgate.net/publication/265379709_Kinetic_Modeling_of_the_Pyrolysis_of_Biomass.
- [35] A. Bieniek, M. Reinmöller, F. Küster, M. Gräbner, W. Jerzak, and A. Magdziarz, "Investigation and modelling of the pyrolysis kinetics of industrial biomass wastes," *J Environ Manage*, vol. 319, p. 115707, Oct. 2022, doi: 10.1016/j.jenvman.2022.115707.
- [36] S. Sunphorka, B. Chalermssinsuwan, and P. Piumsombon, "Artificial neural network model for the prediction of kinetic parameters of biomass pyrolysis from its constituents," *Fuel*, vol. 193, pp. 142-158, Apr. 2017, doi: 10.1016/j.fuel.2016.12.046.
- [37] T. Xie, R. C. Wei, C. Z. Gong, and J. Wang, "Thermal Oxidative Decomposition of Soybean Straw: Thermo-Kinetic Analysis via Thermogravimetric Analysis and Artificial Neural Networks," *IOP Conf Ser Earth Environ Sci*, vol. 581, no. 1, p. 012019, Nov. 2020, doi: 10.1088/1755-1315/581/1/012019.
- [38] A. Hai *et al.*, "Valorization of groundnut shell via pyrolysis: Product distribution, thermodynamic analysis, kinetic estimation, and artificial neural network modeling," *Chemosphere*, vol. 283, p. 131162, Nov. 2021, doi: 10.1016/j.chemosphere.2021.131162.
- [39] L. Dong, R. Wang, P. Liu, and S. Sarvazizi, "Prediction of Pyrolysis Kinetics of Biomass: New Insights from Artificial Intelligence-Based Modeling," *International Journal of Chemical Engineering*, vol. 2022, pp. 1-8, Mar. 2022, doi: 10.1155/2022/6491745.
- [40] S. T. Aly, I. A. Ibrahim, and M. F. Abadir, "Kinetics of Pyrolysis of Date Kernels," *Int J Eng Adv Technol*, vol. 9, no. 3, pp. 930-935, Feb. 2020, doi: 10.35940/ijeat.C5419.029320.
- [41] M. Raza and B. Abu-Jdayil, "Synergic interactions, kinetic and thermodynamic analyses of date palm seeds and cashew shell waste co-pyrolysis using Coats-Redfern method," *Case Studies in Thermal Engineering*, vol. 47, p. 103118, Jul. 2023, doi: 10.1016/j.csite.2023.103118.
- [42] ASTM International, "ASTM C136/C136M Standard Test Method for Sieve Analysis of Fine and Coarse Aggregates," *ASTM Standard Book*, 2019.
- [43] S. Vyazovkin, "Kissinger Method in Kinetics of Materials: Things to Beware and Be Aware of," *Molecules*, vol. 25, no. 12, p. 2813, Jun. 2020, doi: 10.3390/molecules25122813.
- [44] N. Koga and J. šesták, "Further aspects of the kinetic compensation effect," *Journal of Thermal Analysis*, vol. 37, no. 5, 1991, doi: 10.1007/BF01932804.
- [45] D. Rammohan, N. Kishore, and R. V. S. Uppaluri, "Reaction Kinetics of Non-isothermal Pyrolysis of Tube Waste in Thermogravimetric Analyzer," in *Sustainable Energy Generation and Storage*, Singapore: Springer Nature Singapore, 2023, pp. 185-193. doi: 10.1007/978-981-99-2088-4_15.
- [46] J. Li *et al.*, "Comparative Study on Pyrolysis Kinetics Behavior and High-Temperature Fast Pyrolysis Product Analysis of Coastal Zone and Land Biomasses," *ACS Omega*, vol. 7, no. 12, pp. 10144-10155, Mar. 2022, doi: 10.1021/acsomega.1c06363.
- [47] O. A. Montesinos López, A. Montesinos López, and J. Crossa, "Fundamentals of Artificial Neural Networks and Deep Learning," in *Multivariate Statistical Machine Learning Methods for Genomic Prediction*, Cham: Springer International Publishing, 2022, pp. 379-425. doi: 10.1007/978-3-030-89010-0_10.
- [48] I. M. S. Anekwe, "Artificial Intelligence Applications in Solar Photovoltaic Renewable Energy Systems," 2023, pp. 47-86. doi: 10.21741/9781644902530-3.
- [49] J. Arcenegui-Troya, P. E. Sánchez-Jiménez, A. Perejón, and L. A. Pérez-Maqueda, "Determination of the activation energy under isothermal conditions: revisited," *J Therm Anal Calorim*, vol. 148, no. 4, pp. 1679-1686, Feb. 2023, doi: 10.1007/s10973-022-11728-3.
- [50] I. Bakhattar *et al.*, "Physicochemical characterization, thermal analysis and pyrolysis kinetics of lignocellulosic biomasses," *Biofuels*, vol. 14, no. 10, pp. 1015-1026, Nov. 2023, doi: 10.1080/17597269.2023.2201732.
- [51] Y. Li *et al.*, "Pyrolysis kinetics and thermodynamic parameters of bamboo residues and its three main components using thermogravimetric analysis," *Biomass Bioenergy*, vol. 170, p. 106705, Mar. 2023, doi: 10.1016/j.biombioe.2023.106705.

- [52] J. Cheng, S. C. Hu, G. T. Sun, Z. C. Geng, and M. Q. Zhu, "The effect of pyrolysis temperature on the characteristics of biochar, pyrolytic acids, and gas prepared from cotton stalk through a polygeneration process," *Ind Crops Prod*, vol. 170, 2021, doi: 10.1016/j.indcrop.2021.113690.
- [53] N. M. Noor, A. Shariff, N. Abdullah, and N. S. M. Aziz, "Temperature effect on biochar properties from slow pyrolysis of coconut flesh waste," *Malaysian Journal of Fundamental and Applied Sciences*, vol. 15, no. 2, 2019, doi: 10.11113/mjfas.v15n2.1015.
- [54] K. Wystalska and A. Kwarciak-Kozłowska, "The Effect of Biodegradable Waste Pyrolysis Temperatures on Selected Biochar Properties," *Materials*, vol. 14, no. 7, p. 1644, Mar. 2021, doi: 10.3390/ma14071644.